

Empirical Estimates of NS-NS Merger Rates in the Galaxy

M. Evans, S.B. Anderson, K. Blackburn, A. Lazzarini, and T.A. Prince
LIGO Laboratory, California Institute of Technology, Pasadena, CA 91125 USA

Binary neutron star (NS-NS) systems with short orbital periods evolve by emission of gravitational waves and eventually coalesce. We estimate the rate of such mergers in our Galaxy from the observations of known NS-NS binaries that have merger time scales shorter than the Hubble time. We also explore the sensitivity of the estimates to assumptions about the initial position and velocity distributions.

1 Introduction

The rate of NS-NS mergers is potentially important for several fields of observational astrophysics including gravitational wave and γ -ray burst astronomy. For gravitational wave detection, NS-NS mergers are a promising source. Their gravitational waveforms can be computed accurately, and there are several progenitor systems known in our Galaxy.

Estimates of the NS-NS mergers fall into two classes. Empirical estimates extrapolate from the small number of detected NS-NS binaries to the population of the galaxy as a whole. Population synthesis estimates use scenarios for close binary evolution to estimate the number of massive binaries that end their evolution as a close NS-NS pair. In this paper, we concentrate on empirical estimates. Previous empirical estimates include those of Phinney[12], Narayan et al.[9], Curran & Lorimer [5], van den Heuvel and Lorimer [15], Stairs et al. [13] and Arzoumanian et al.[1]. Most of these estimates were made using a specific set of assumptions about the spatial and velocity distributions at birth. Our work was motivated by the desire to explore the sensitivity of the estimates to the birth distribution assumptions, particularly the dependence on recoil velocity of the NS-NS binary. To explore this dependence, we found that we needed to employ a different methodology from previous studies in order to self-consistently treat the detectability and evolution of the pulsar and binary systems.

Three NS-NS systems have been detected that will coalesce in less than a Hubble time: PSR B1913+16, PSR B1534+12, and PSR B2127+11C. In this paper, we consider these individual systems as stochastic events which represent a sampling from an underlying ensemble of identical systems. Our task is to estimate the size of the ensemble from the number of individual systems detected. Obviously, the accuracy of the estimate is limited by the extremely small sample of systems. One of the systems, PSR B2127+11C, is a member of a globular cluster and thus is representative of an interesting, but small, population. It contributes negligibly to the total merger rate in the Galaxy and we do not consider it further in this paper.

2 Methodology

The galactic merger rate of NS-NS systems can be estimated by determining the birth rate required to make the detection of the two known NS-NS systems have maximum likelihood. The maximum likelihood birth rate is given by $\dot{n} = N_{det}/\tau_{life} P_{vis}$, where N_{det} is the number of systems of a given type which have been observed, τ_{life} is the total lifetime of a system in the ensemble and P_{vis} is the probability of observing a member of the ensemble during its lifetime. P_{vis} is given by

$$P_{vis} = \int_{\vec{x}} \int_0^{\tau_{life}} P_{det}(t_{age} = t, \vec{x}_{init} = \vec{x}) P_{age}(t_{age} = t) P_{init}(\vec{x}_{init} = \vec{x}) dt d\vec{x}, \quad (1)$$

where $P_{det}(t_{age} = t, \vec{x}_{init} = \vec{x})$ is the probability of detecting a system with age t_{age} and birth position and velocity \vec{x}_{init} , $P_{age}(t_{age} = t)$ is the probability density function for having systems of age t_{age} , and $P_{init}(\vec{x}_{init} = \vec{x})$ is the probability density of initial conditions. For systems which will merge in less than a Hubble time, the birth rate is equal to the death rate and both are time independent. This implies that $P_{age}(t_{age} = t) = \frac{1}{\tau_{life}}$, and $P_{vis} = \langle \tau_{vis} \rangle / \tau_{life}$, where τ_{vis} is defined by

$$\tau_{vis} \equiv \int_0^{\tau_{life}} P_{det}(t_{age} = t, \vec{x}_{init} = \vec{x}) dt \quad (2)$$

and the expectation value, $\langle \tau_{vis} \rangle$, is over initial conditions. τ_{vis} for a given system can be intuitively interpreted as the duration for which that system is “visible” to pulsar surveys.

This analysis results in a simple birth rate estimate for an ensemble of identical systems, $\dot{n} = N_{det}/\langle \tau_{vis} \rangle$. Since all NS-NS systems are clearly not identical, our rate estimate will include a population factor, $0 \leq f_d \leq 1$, which is a measure of how representative a given observed system is of the galactic population. While $f_d \sim 0.1$ has been used by other authors, we will leave this as a free parameter in our analysis (c.f. Curran & Lorimer [5], Arzoumanian et al. [1]). Including this factor in the birth rate estimate and summing over observed objects results in an estimate of the total galactic birth rate of NS-NS systems,

$$\dot{N} = \sum_i \frac{1}{(f_d \langle \tau_{vis} \rangle)_i}. \quad (3)$$

The approximation to $\langle \tau_{vis} \rangle$ most frequently used in the literature is $\langle \tau_{vis} \rangle = V_{det} \tau_{obs} / V_{gal}$, where V_{gal} is the volume of the galaxy, V_{det} is the volume in which similar systems could have been detected, and τ_{obs} is the observable lifetime of the system (originally taken to be the characteristic age of the pulsar plus the binary merger time). The approximations found in most of the literature have failed to account for the dependence of the spatial distribution, the period, and the luminosity, on the age of the system. In fact it is not possible to self-consistently decouple system evolution from phase space evolution when determining $\langle \tau_{vis} \rangle$. Instead of trying to decouple the components of $\langle \tau_{vis} \rangle$, we model the evolution of NS-NS systems as they move in the galactic potential and numerically perform the integral in equation (2) for each model system. We then use a combination of Monte Carlo integration and analytic integration to produce the expectation value $\langle \tau_{vis} \rangle$. Some of the details of this model are discussed in the following section.

3 Model Assumptions

Birth spatial and velocity distributions. To investigate the sensitivity of the NS-NS merger rate estimates to input assumptions, we compared results using several spatial and

velocity distributions. NS-NS systems were assumed to be born in the galactic disk. Among the spatial distributions we used were those of Johnston [7], and Binney et al.[2] with various exponential radial scales. The recoil velocity distributions are not well known. We were guided by the results of Fryer and Kalogera [6] which indicate that the two known Galactic disk systems, PSR B1913+16 and PSR B1534+12, have binary recoil velocities greater than about 200 km/s, but probably less than about 400 km/s. We compared Maxwellian distributions and delta function distributions with a variety of recoil velocities. We found (see Section 4, Figure 1) that the merger rate estimates are not highly sensitive to the details of plausible spatial or velocity distributions.

Galactic gravitational potential. In order to determine τ_{vis} for a given model system, its position and velocity are evolved as it moves in the galactic potential. We used the potential suggested by Paczynski [10] which contains terms representing the bulge, disk and halo. We performed phase space evolution in this potential with a numerical integration algorithm.

Spin evolution. We approximate the evolution of the pulsar spin, Ω , according to a conventional model for pulsar rotation frequency evolution. This model assumes that the time derivative of the rotation frequency is proportional to some power of the rotation frequency, $\dot{\Omega} = -K_{\dot{\Omega}}\Omega^{n_b}$, where n_b is the braking index.

Given an age estimate for a pulsar, its initial spin period can be determined, assuming $n_b \neq 1$, by integrating the expression for $\dot{\Omega}$ to obtain

$$\Omega(t) = \left[K_{\dot{\Omega}}(n_b - 1)(t - t_0) + \Omega(t_0)^{1-n_b} \right]^{\frac{1}{1-n_b}}. \quad (4)$$

Luminosity evolution. For the purposes of this calculation we assume that the luminosity of a pulsar at a given frequency is proportional to its total rate of rotational kinetic energy loss, i.e. $\dot{E} = K_{\dot{E}}\Omega\dot{\Omega}$. and $L = -K_L\dot{E}$, where $K_{\dot{E}}$ and K_L are constants of proportionality. Combining the equations for $\dot{\Omega}$, \dot{E} , and L yields the dependence of luminosity of the pulsar on rotation frequency,

$$L \propto \Omega^{n_b+1}. \quad (5)$$

Radio survey characteristics. The surveys considered herein were characterized by their central frequency f_c , channel bandwidth df , number of channels $N_{channel}$, minimum flux for close long period pulsars S_{min0} , and sky coverage. Our list of applicable surveys is taken from Cordes [4]. References for the surveys are given therein. The sky coverage of a survey is accounted for by a factor P_{area} , which takes on a ‘‘Fractional Coverage’’ value inside the survey’s sky patch, and zero elsewhere. (In the model implementation the edges of the sky patch are softened slightly to avoid a discontinuity, which can make numerical integration difficult.)

Galactic electron model. The visibility of a pulsar is affected by the presence of free electrons in the interstellar medium. Realistic galactic electron density models must include significant non-axisymmetric structure and generally require numerical integration to determine the heliocentric dispersion measure (DM) and scattering measure (SM) of a pulsar. This level of detail is computationally expensive, so we used two axisymmetric models, rough lower and upper bounds on the Taylor and Cordes[14] model, to determine its importance.

Dispersion and scattering both alter the detectability of a pulsar by broadening the pulse profile as observed in a given frequency channel of the receiver. The minimum detectable flux

varies with pulse width as

$$S_{min} = S_{min0} \left(\frac{w}{P-w} \right)^{1/2}, \quad (6)$$

where w is the pulse width, P is the pulse period and S_{min0} is the nominal minimum detectable flux. [3] For w we used the usual scaling, $w = \sqrt{w_{PSR}^2 + \tau_{DM}^2 + \tau_{SM}^2 + \tau_{sample}^2}$, with standard values for the pulse width, w_{PSR} , dispersion and scattering time scales, τ_{DM} and τ_{SM} , and sampling time, τ_{sample} .

The strong scattering regime applies to all but the closest ($d < 100pc$) pulsars.[4] In this regime interstellar scintillation can play an important role in pulsar detection. We have included the effects of scintillation on the probability of detecting a pulsar, P_{flux} . This correction depends on the specifics of the survey (e.g. S_{min} and df) and the scattering measure to the pulsar (Cordes [4]). The product of P_{flux} and P_{area} is P_{det} , the detection probability in equation (1).

Doppler shift effects. Because of gravitational radiation, the orbital period of NS-NS systems decrease with time. During the orbital evolution, both the semi-major axis, a , and the orbital eccentricity, e , decrease. [11]

The orbital evolution will effect the detectability of a radio pulsar in a NS-NS system: when the orbital period becomes sufficiently small, the change in the pulse frequency due to variations in the line of sight velocity will be large enough to smear the detected power across several frequency bins, thus decreasing the effective signal-to-noise of the observation. This effect is most significant for the higher harmonics of the radio pulsations.

It is straightforward to quantify Doppler effects within the framework of the mean visibility time formalism. We treat short-orbital period accelerations as reducing the effective luminosity of the radio pulsar in the NS-NS system. Indeed, some power will be present at the instantaneous pulse period of the observation even for rather large accelerations. The higher harmonics will exhibit decreased effective luminosity earliest in the orbital evolution, and then the fundamental will show such effects as the orbit further decays. The magnitude of the effect is also dependent on the inclination of the orbital plane relative to the line-of-sight.

The phase of the pulsed emission can be expressed as

$$\phi = \phi_0 + \omega_0 t + \dot{\omega}_0 \frac{t^2}{2} + \dots, \quad (7)$$

where ω_0 and $\dot{\omega}_0$ are the apparent pulsar frequency and frequency derivative at the beginning of the observation. Neglecting the small intrinsic frequency derivative of the pulsar, the frequency derivative is to first order $\dot{\omega}_0 = a_{radial}\omega_0/c$, where a_{radial} is the acceleration due to the orbital motion. Consequently, the phase error compared to a constant frequency model for an observation interval, $[-T_{obs}/2, T_{obs}/2]$ is approximately $\delta\phi \sim a_{radial}\omega_0 T_{obs}^2/16c$. The effective coherence time is

$$t_{coh} = \sqrt{\frac{8P_{puls} \delta\phi_{max} c}{\pi a_{radial}}}, \quad (8)$$

where $\delta\phi_{max}$ is the maximum allowed phase error for coherence to be maintained.

We now choose a phenomenological luminosity law, $L = L_0 \left(1 - e^{-t_{coh}/T_{obs}} \right)$, where L_0 is the apparent luminosity of the pulsar in the case of vanishing orbital acceleration. The luminosity L approaches L_0 for t_{coh} significantly longer than T_{obs} , and approaches $L_0 t_{coh}/T_{obs}$ for t_{coh} significantly shorter than T_{obs} .

The results of using the phenomenological luminosity reduction have been checked against exact calculations for circular orbits.[8] They compare well over a wide range of orbital accelerations and therefore we feel confident that the results extend to the more general case of non-circular orbits.

4 Results

For the distributions considered here the dependence on birth position distribution is fairly weak (see Figure 1a). Since all reasonable birth distributions have their peak well inside the galactocentric radius of the sun, this is not expected to change as birth distribution models are refined. The Johnston [7] distribution is used as the fiducial distribution. In most cases it produces $\langle\tau_{vis}\rangle$ values which are large compared with those of other distributions and thus serves to generate a soft lower bound on the NS-NS birth rate. Figure 1 also indicates a moderate dependence on birth velocity for velocities between 200 and 400 km/s, typical of PSR1913+16 and PSR1534+12[6].

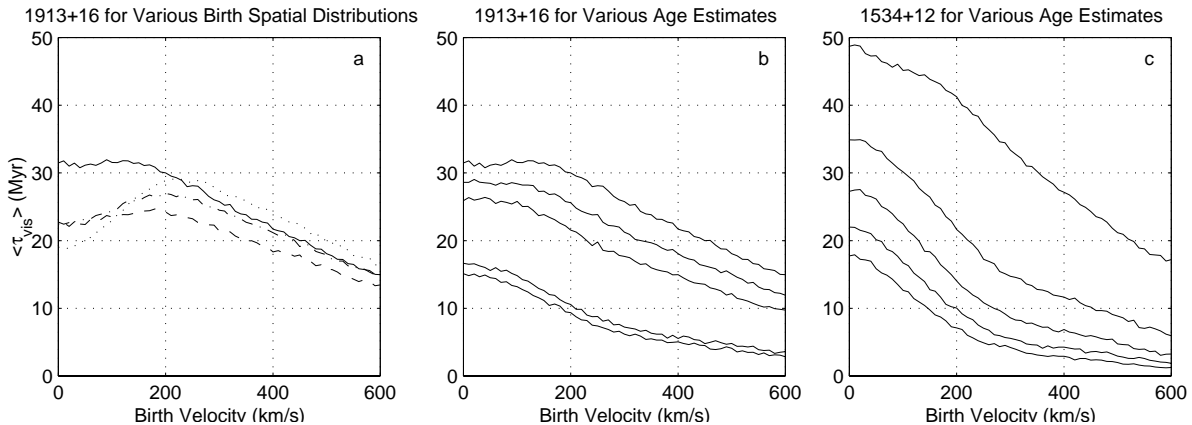


Figure 1: (a) $\langle\tau_{vis}\rangle$ for 1913+16 is shown for various birth spatial distributions. The distributions used are that suggested by Johnston [7] —, a $4.5kpc$ exponential — —, a $3.5kpc$ exponential — · —, and a $2.5kpc$ exponential · · · · (b) $\langle\tau_{vis}\rangle$ for 1913+16 is shown for various age estimates. From bottom to top they are 0, 10, 60, 70 and 80 Myr. This spans the allowed values suggested by Arzoumanian et al.[1]. (c) $\langle\tau_{vis}\rangle$ for 1534+12 is shown for various age estimates. From bottom to top they are 0, 50, 100, 150 and 210 Myr.

There is also relatively little dependence of $\langle\tau_{vis}\rangle$ on braking index. Lowering the braking index to $n_b = 2.5$ alters the $\langle\tau_{vis}\rangle$ of a NS-NS system by about 10% in all but the closest binaries. The canonical magnetic dipole value, $n_b = 3.0$, is used as the fiducial in this paper.

Unlike the two previously mentioned inputs, the dependence of $\langle\tau_{vis}\rangle$ on the assumed ages of the two example systems is fairly strong (see Figure 1b and c). The older a system is assumed to be, the more initial angular momentum it has to radiate away. Thus, even if the characteristic age of the system is small compared to its merger time, the assumed age of the system can greatly effect $\langle\tau_{vis}\rangle$. The fiducial ages used in this paper (e.g. for Table 1) are 80 Myr for PSR B1913+16 and 210 Myr for PSR B1534+12. Again, these values are chosen because they are plausible [1] and serve to produce a lower bound NS-NS birth rate estimate.

5 Discussion

There are at least two items that have been left largely unaddressed: beaming and the population factor f_d . Beaming amounts to an overall reduction in the probability of detecting a pulsar at any given time, and thus is simply a multiplicative reduction of $\langle\tau_{vis}\rangle$. For the sake of producing a numerical result which can be compared with that of previous authors, a beaming fraction of one third will be used, i.e. $f_b = 1/3$.

The parameter, f_d , depends on the characteristics of the galactic NS-NS population, for instance, the luminosity distribution. Unfortunately, f_d is rather poorly constrained. For the purpose of numerical comparison $f_d = 0.1$ will be used, which is consistent with the correction made in previous literature for the low-luminosity tail of the pulsar distribution.

Combining f_d and f_b effectively increases the rate estimate by a factor of 30. To arrive at a final rate estimate, a birth velocity distribution must be convolved with the $\langle\tau_{vis}\rangle$ vs. birth velocity function for each NS-NS system (see Figure 1b and c). Table 1 gives NS-NS birth rate estimates for two birth velocity distributions. For comparison, we also reproduce two recent estimates of the merger rate (assuming $f_d = 0.1$ and $f_b = 1/3$ in both cases).

Table 1: NS-NS Birth Rate Estimates

Birth Velocity Distribution	Rate (Myr ⁻¹)
Maxwellian with $\sigma_v = 190$ km/s	2.1
Delta function at 200 km/s	1.7
Stairs et. al [13]	3.3
Arzoumanian et al.[1]	6.4

Acknowledgments

We thank V. Kalogera for interesting discussions. This is work funded in part by NSF PHYS-9210038 and NASA NAG-5-3239. This paper has been designated LIGO-P990025-00-R.

References

1. Z. Arzoumanian, J.M. Cordes, & I. Wasserman, submitted to ApJ, 1998.
2. J. Binney, O. Gerhard, & D. Spergel, MNRAS **288**, 365 (1997)
3. F. Camilo, D.J. Nice, & J.H. Taylor, ApJ **461**, 812 (1996)
4. J.M. Cordes & D.F. Chernoff ApJ **482**, 971 (1997)
5. S.J. Curran & D.R. Lorimer, MNRAS **276**, 347 (1995)
6. C. Fryer & V. Kalogera, ApJ **489**, 244 (1997)
7. S. Johnston, MNRAS **268**, 595 (1994)
8. H. M. Johnston & S. R. Kulkarni, ApJ **368**, 504 (1991)
9. R. Narayan, T. Piran, & A. Shemi, ApJ **379**, L17 (1991)
10. B. Paczynski, ApJ **348**, 485 (1990)
11. P. C. Peters, Phys. Rev. B **136**, 1124 (1964)
12. E.S. Phinney, ApJ Letters **380**, L17–L21 (1991)
13. I.H., Stairs, *et al* ApJ **505**, 352 (1998)
14. J.H. Taylor & J.M. Cordes, ApJ **411**, 674–684 (1993)
15. E. P.J. Van Den Heuvel & D.R. Lorimer, MNRAS **283**, L37–L40 (1996)

Note 1, Linda L Turner, 04/15/99 01:49:01 PM
LIGO-P990021-00-D